Antitumor Agents (1)

DOI: 10.1002/anie.201208373

The Cytotoxicity of Duocarmycin Analogues is Mediated through Alkylation of DNA, not Aldehyde Dehydrogenase 1: A Comment**

Moana Tercel, Sarah P. McManaway, Euphemia Leung, H. D. Sarath Liyanage, Guo-Liang Lu, and Frederik B. Pruijn**

activity-based protein profiling · antitumor agents · biological activity · DNA damage · duocarmycin

Duocarmycin SA (**1**) is one member of a small group of natural products that are notable for their extreme cytotoxicity, which is generally believed to be a consequence of DNA alkylation.[1] Much evidence has been advanced to support a mechanism of action involving sequence-selective reaction at N3 of adenine at the base of the minor groove; this evidence includes, for example, the isolation of adducts such as **2** following thermal depurination of alkylated DNA (Scheme 1).[2] It was recently reported that duocarmycin analogues (*S*,*S*)-**3** and (*S*)-**4**, bearing synthetic seco variants of the alkylating subunit (with the same enantiomeric form as the natural products), are able to alkylate aldehyde dehydrogenase 1 (ALDH1A1), and indeed these compounds were described as selective and potent inhibitors of ALDH1A1 in A549 lung cancer cells.[3] The evidence for ALDH1A1 alkylation included activity-based protein profiling (ABPP) of the "clickable" analogue (*S*)-**4**, MS/MS sequencing of recombinant ALDH1A1 alkylated with (*S*)-**4**, and competition between (*S*,*S*)-**3** and (*S*)-**4** in the ABPP assay. ALDH1A1 inhibition was investigated by using recombinant enzyme and A549 cell lysates rather than living cells, thereby making it difficult to relate the observed inhibitory potency to cytotoxicity. Nevertheless, the authors concluded that inhibition of ALDH1A1 contributes to the cytotoxicity of the duocarmycin family of compounds, and that in particular for (*S*,*S*)-**3** this inhibition is likely to be the preferred mechanism of action. This inference was based on the claim that (*S*,*S*)-**3** does not bind to or alkylate DNA, citing previous work from the same group that failed to detect an interaction between (*S*,*S*)-**3** and oligonucleotides by circular dichroism, or evidence for significant interstrand crosslinks by mass spectrometry.[4] These observations stand in marked contrast to earlier studies in which dimers of a similar structure to (*S*,*S*)-**3** were shown to crosslink DNA and a correlation between crosslinking ability and cytotoxicity was demonstrated.[5] Prompted by these observations we have investigated (*S*,*S*)-**3** and (*S*)-**4** and find that while these compounds are indeed capable of alkylating ALDH1A1 (and other proteins), their cytotoxicity, including the marked picomolar toxicity of (*S*,*S*)-**3**, can be attributed to the alkylation of DNA.

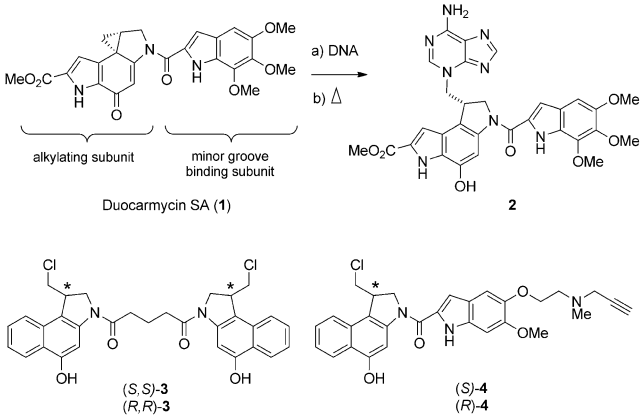

Scheme 1. Structures of duocarmycin SA, its N3 adenine adduct, and the seco duocarmycin analogues **3** and **4**.

(*S*,*S*)-**3** and (*S*)-**4** and their previously unreported enantiomers (*R*,*R*)-**3** and (*R*)-**4** were prepared using slight modifications of the published procedure.[3,6] To investigate if (*S*,*S*)-**3** can alkylate DNA a solution of this compound (0.1 μM) was incubated with calf thymus DNA (ctDNA, 250 μM in base pairs) at 37 °C in aqueous buffer containing 10% dimethylacetamide (DMA; Figure 1). Under these conditions and in the absence of DNA (*S*,*S*)-**3** is completely converted via the monocyclopropyl intermediate [(*S*,*S*)-**S3** in the Supporting Information] to the biscyclopropyl compound (*S*,*S*)-**5** over about 3 h; the products were characterized by LC–MS and UV absorbance spectra.[6] Incubation with DNA

[*] Dr. M. Tercel, S. P. McManaway, Dr. E. Leung, H. D. S. Liyanage, Dr. G.-L. Lu, Dr. F. B. Pruijn
Auckland Cancer Society Research Centre
Faculty of Medical and Health Sciences
The University of Auckland
Private Bag 92019, Auckland 1142 (New Zealand)
E-mail: m.tercel@auckland.ac.nz
f.pruijn@auckland.ac.nz

[**] This research was funded by the Foundation for Research, Science and Technology, NZ, and the Auckland Division of the Cancer Society of New Zealand. The authors thank Dr. Nicholas Lloyd for technical assistance.

Supporting information for this article is available on the WWW under http://dx.doi.org/10.1002/anie.201208373.

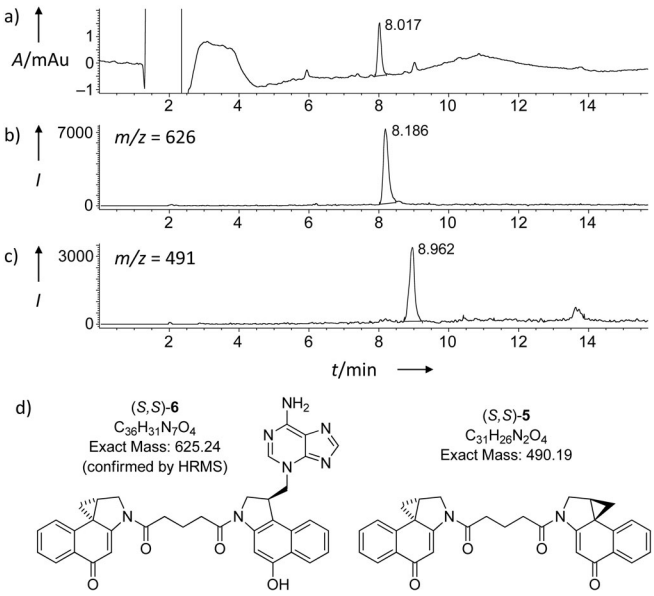

Figure 1. Interaction of (*S*,*S*)-**3** with calf thymus DNA. (*S*,*S*)-**3** (0.1 μM) was incubated with excess ctDNA [250 μM base pairs in TE buffer (10 mM Tris buffer containing 1 mM EDTA, pH 7.4) with 10% DMA, 37 °C, 23 h], the DNA precipitated and heated (TE buffer, 90 °C, 10 min) to induce thermal depurination of alkylated bases, and the supernatant analyzed by LC–MS (positive electrospray ionization) after reprecipitation of the DNA. a) Chromatogram monitoring absorbance (*A*) at 320 nm. b, c) Extracted ion chromatograms (EIC) at $m/z = 626$ and 491 respectively. *I* = extracted ion intensity. Note that because of the configuration of the absorbance and mass detectors there is an off-set of about 0.17 min between the two signals. d) Structures assigned to the peaks observed in (b) (*S*,*S*)-**6** and (c) (*S*,*S*)-**5**.

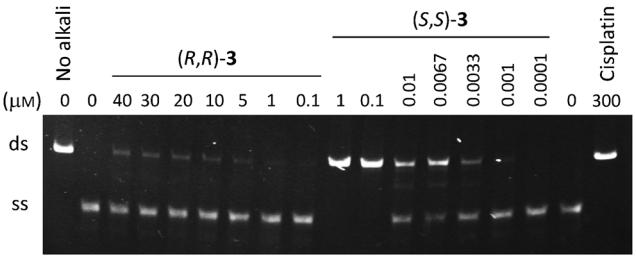

Figure 2. Crosslinking of DNA. (*S*,*S*)-**3** and (*R*,*R*)-**3** were incubated at the concentrations shown with linearized F527V5 plasmid (2.25 nM, 5111 base pair length, 11.5 μM in base pairs) for 24 h at 37 °C. The samples were treated with alkali to induce strand separation and run on a 0.8% agarose gel (45 V, 2 h). The DNA was visualized by staining with ethidium bromide. ds = double-stranded DNA; ss = single-stranded DNA.

was allowed to proceed for 23 h, and the DNA precipitated by the addition of acetonitrile. Analysis of the supernatant failed to detect any (*S*,*S*)-**3** or spirocyclized product, thus indicating that all of the material derived from (*S*,*S*)-**3** had precipitated with the DNA. Heating the DNA (90 °C, 10 min) released acetonitrile-soluble products, two of which were identified as (*S*,*S*)-**5** and the adenine adduct (*S*,*S*)-**6** (Figure 1). The latter was characterized by LC–MS and absorbance spectroscopy, and the molecular formula was confirmed by HRMS analysis of a sample purified by HPLC. Thermal depurination of N3-alkylated adenine from DNA has been widely observed with duocarmycin analogues in the past, but has not been reported for any dimeric structure. Duocarmycin DNA alkylation is known to be reversible, with the rate sensitive to several factors including the structure of the duocarmycin analogue.[2a,7] It is possible that (*S*,*S*)-**3**, which lacks a minor-groove-binding indole side chain, is prone to the reversible reaction, thus explaining why (*S*,*S*)-**5** was observed after but not before depurination, and why only traces of a putative bisadenine adduct could be detected by LC–MS.

The ability of (*S*,*S*)-**3** to crosslink DNA was investigated by using linearized plasmid DNA in an alkaline gel electrophoresis assay[8] (Figure 2). Crosslinking is demonstrated by the appearance of double-stranded (ds) DNA under otherwise denaturing conditions, and could be detected with (*S*,*S*)-**3** at concentrations as low as 1 nM, corresponding to less than one molecule of (*S*,*S*)-**3** per segment of linear DNA under the assay conditions. (*R*,*R*)-**3** also induced crosslinking but at much higher concentrations, with the differential crosslinking ability being on the order of 1000-fold or more.[6] Thus there is clear evidence that (*S*,*S*)-**3**, in contrast to the previous report, can both alkylate and crosslink DNA, and is in fact a very efficient DNA-crosslinking agent.

Cytotoxicity of the enantiomers of **3** and **4** was determined by inhibition of proliferation after 4 h exposure to the compounds in a panel of six human tumor cell lines (Figure 3). The activities of (*S*)-**4** and (*S*,*S*)-**3** in A549 (IC_{50} values of 6.3 and 0.20 pM respectively) were very similar to those reported[3] (14 and 0.11 pM) despite the different compound exposure times. The results emphasize the cytotoxic potency of (*S*)-**4** and especially (*S*,*S*)-**3** and the striking effect of inverting the optically active center: (*S*)-**4** is on average 300 times more toxic than (*R*)-**4**, while for **3** the IC_{50} values of the *S*,*S* enantiomer are on average 4000-fold lower than those of the *R*,*R* enantiomer across the cell line panel,[6] that is, the difference is of the same order of magnitude as the differential DNA crosslinking ability of this pair of enantiomers. Cytotoxicity was also determined in a pair of Chinese hamster ovary cell lines that differ only in the presence or absence of the gene encoding Rad51d. This protein is critical for the repair of DNA lesions by homologous recombination,[9] and hypersensitivity to the repair-defective cell line has been observed with several classes of DNA alkylating agents, including amino derivatives of the duocarmycins.[10] All four compounds in the present study were significantly more sensitive to the repair-deficient line by factors of 6- to 19-fold.[6] Further, when cytotoxicities were compared across all eight cell lines investigated, highly significant correlations for all pair-wise compound comparisons ($P < 0.007$) were observed.[6] Together these results implicate a common mechanism of action for the enantiomers of **3** and **4**, one involving alkylation of DNA.

The panel in Figure 3 was chosen to include cell lines with a range of expression of ALDH1A1, based on RNA abundance from microarray data for five of the six lines,[11] and the finding that MCF7 contains little or no ALDH1A1.[12] The panel was subjected to ABPP using (*S*)-**4** essentially as described[3] and ALDH1A1 was identified by Western blot-

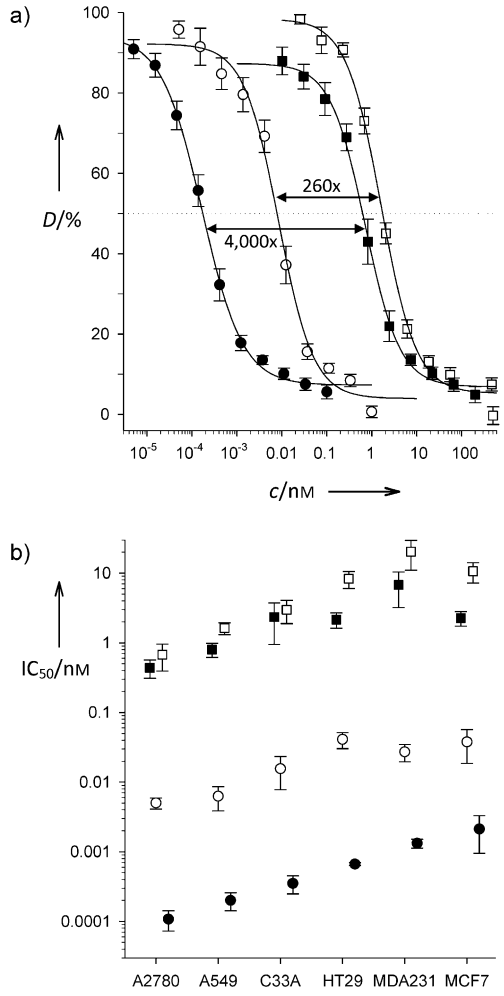

Figure 3. Cytotoxicity of the enantiomers of **3** and **4** in human tumor cell lines, as determined by inhibition of proliferation. Cell monolayers were exposed to the compounds for 4 h, and proliferation was measured 5 days later. a) Cell density of A549 cells compared to untreated control cells; *D*: cell density as a percentage of intra-experiment control; *c*: compound concentration; data points ± standard error of the mean (SEM) for 6 determinations; solid lines: fitted four-parameter logistic regressions for each compound. b) Cytotoxicity in a cell line panel; IC_{50}: concentration required to inhibit cell proliferation by 50%. (*S*,*S*)-**3** (●); (*R*,*R*)-**3** (■); (*S*)-**4** (○); (*R*)-**4** (□).

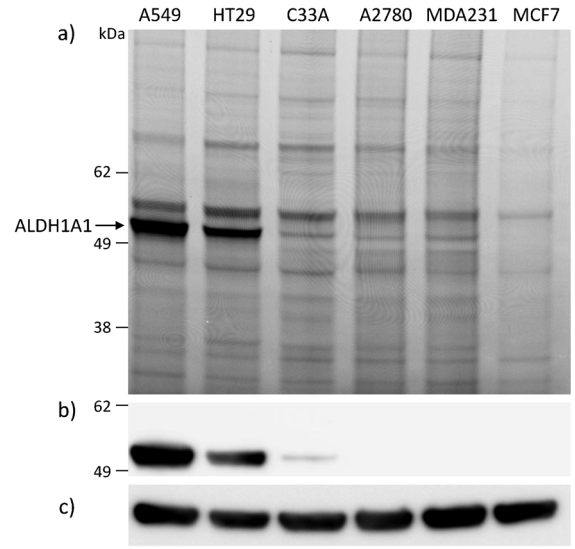

Figure 4. ABPP using (*S*)-**4** in a panel of human tumor cell lines. Cells were exposed to (*S*)-**4** (3 μM, 4 h) and the cytosolic fraction of the cell lysates was labeled with a tetramethylrhodamine (TAMRA) fluorophore in a click reaction. Samples containing 25 μg protein were run on a polyacrylamide gel and the fluorescence was visualized using a laser scanner (a). Western blotting was performed to identify ALDH1A1 (b) and actin (c) to confirm equal protein loading.

ting (Figure 4). Fluorescent labeling of A549 cytosolic proteins was qualitatively similar to that reported,[3] but ALDH1A1 was a prominent band only in this cell line and in HT29, the two lines that exhibit the highest levels of ALDH1A1 in this panel.[6] A549 was notable in the original microarray analysis in having the largest amount of ALDH1A1 RNA amongst 23 diverse human tumor cell lines, including three other representatives of non-small cell lung cancer. In other words, selectivity for alkylation of ALDH1A1 by (*S*)-**4** is only apparent in cells with an unusually high abundance of this protein. Importantly, a comparison between Figures 3 and 4 shows that there is no correlation between cytotoxicity and either ALDH1A1 abundance or fluorescent labeling by (*S*)-**4**. As an example A2780 is more sensitive than A549 to (*S*)-**4** (and to the other three compounds) but exhibits little if any fluorescent labeling of ALDH1A1 and no detectable protein by Western blotting.

A comparison of the ABPP activity of the enantiomers of **4** (Figure 5 a) shows approximately 10-fold stronger labeling

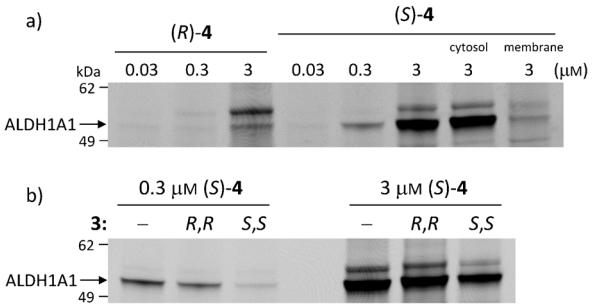

Figure 5. Enantioselectivity of the alkylation of ALDH1A1 by **3** and **4** in A549 cells. a) A549 cells were exposed to the enantiomers of **4** (4 h at the concentrations shown); b) A549 cells were exposed to (*S*)-**4** (0.3 or 3 μM, 4 h) in the presence or absence of (*S*,*S*)-**3** and (*R*,*R*)-**3** (3 μM). In both cases cell lysates were labeled with a TAMRA fluorophore and ALDH1A1 was visualized as in Figure 4.

of ALDH1A1 by (*S*)-**4** compared to (*R*)-**4**. This can be seen from the similar band intensities at 3 μM (*R*)-**4** and 0.3 μM (*S*)-**4**, and by a comparison of band densities at both of these concentrations.[6] The enantiomers of **3** were compared by their ability to compete with (*S*)-**4** for fluorescent labeling of ALDH1A1 (Figure 5 b). Again there is more efficient competition by the *S*,*S* enantiomer, but the discrimination is weak, with a differential of only 2- to 3-fold in repeat experiments.[6] Clearly the selectivity of the *S* over the *R* enantiomers for

ALDH1A1 alkylation in A549 cells is much smaller than that observed for cytotoxicity, especially for the enantiomers of **3**.

To assess the ability of **3** and **4** to inhibit aldehyde dehydrogenase in intact cells the Aldefluor flow cytometry assay was employed. In this assay a fluorescent ALDH substrate becomes cell-entrapped after enzymatic activation, with the increase in fluorescence being sensitive to the presence of the selective inhibitor diethylaminobenzaldehyde (DEAB).[13] In lung cancer cell lines a good correlation has been found between Western blotting for ALDH1A1 and the Aldefluor assay.[14] This correlation holds for A549 provided its very high ALDH activity is diluted with an excess of an ALDH-null cell line (MCF7) before addition of the assay substrate.[14] A549 cells were exposed to the enantiomers of **3** and **4** under the conditions of the cytotoxicity assay (4 h, 37 °C), then washed and mixed with a 9-fold excess of MCF7 cells (Figure 6). No effect was observed in the Aldefluor assay

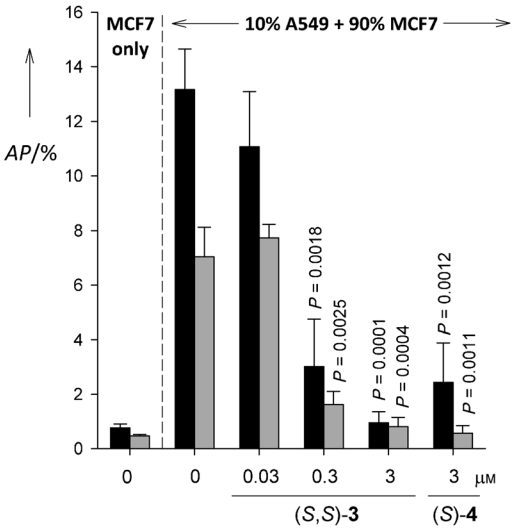

Figure 6. Inhibition of ALDH1A1 in A549 cells as measured by the Aldefluor assay. A549 cells were exposed to (*S*,*S*)-**3** and (*S*)-**4** (4 h, 37 °C), then washed, mixed with MCF7 cells, and subjected to the Aldefluor assay [1.5 μM BODIPY aminoacetaldehyde in the presence or absence of 50 μM diethylaminobenzaldehyde (DEAB), 60 min, 37 °C]. Cells were analyzed by flow cytometry to determine *AP*: the percentage of Aldefluor-positive cells (mean ± SEM for 2–4 determinations). Black bars: no DEAB; gray bars: with DEAB. Statistical significance was assessed relative to the appropriate control with or without DEAB. Representative flow cytometry plots are shown in the Supporting Information.

for (*R*,*R*)-**3** or (*R*)-**4** at 3 μM, while a concentration-dependent inhibition could be seen for the *S* enantiomers (Figure 6). While there was some error in the detection of Aldefluor-positive cells and incomplete inhibition of the signal by DEAB, there was also a clear transition from ALDH1A1 inhibition at 3 μM of (*S*,*S*)-**3** to no effect at 0.03 μM. Dual staining with propidium iodide established that even at 3 μM of (*S*,*S*)-**3** there was no loss of cell viability over the course of the assay.[6] Notably, detectable inhibition of ALDH in intact cells requires concentrations of (*S*,*S*)-**3** and (*S*)-**4** about a million-fold higher than the IC_{50} values of these compounds, thus effectively ruling out any contribution from ALDH inhibition to the observed cytotoxicity.

Finally, the subcellular distribution of the fluorescent signal derived from (*S*)-**4** was investigated by confocal microscopy. A549 cells grown on coverslips were exposed to (*S*)-**4** (1 μM, 4 h), then fixed and permeabilized and subjected to a click reaction with a fluorophore azide. Under these conditions protein labeling as detected by ABPP is predominantly associated with the cytosolic fraction (Figure 5a and Figure S8), but as observed by confocal microscopy the fluorescent signal is entirely colocalized with the nucleus (Figure 7). Similar observations were made with MCF7

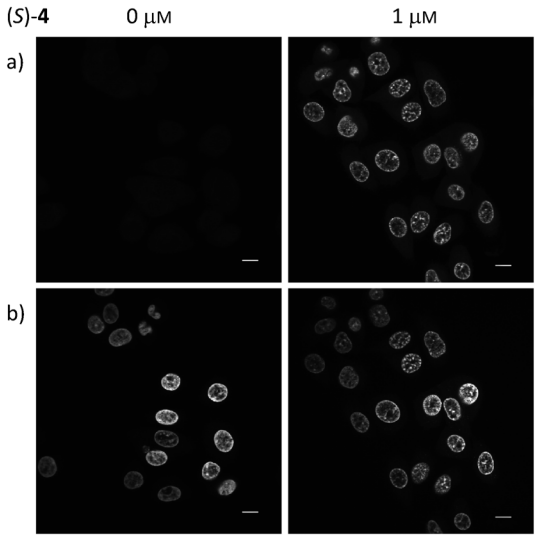

Figure 7. Subcellular localization of the signal associated with (*S*)-**4**. A549 cells grown on coverslips were exposed to (*S*)-**4** (0 or 1 μM, 4 h), then fixed and permeabilized and subjected to a click reaction with Alexa Fluor 647 azide. Cells were also exposed to the nuclear stain Hoechst 33342. Imaging was done by confocal microscopy at 60× magnification. a) Fluorescent signal observed after the click reaction (excitation 635 nm, emission band filter 650/100); b) Hoechst signal (excitation 405 nm, emission band filter 425/50). The scale bar is 10 μm long.

cells.[6] While the relative efficiencies of the click reaction in various subcellular locations are not known, strong nuclear and not cytosolic staining by (*S*)-**4** supports the preferential alkylation of DNA rather than ALDH1A1 or other cytosolic proteins by this compound.

Overall, the data presented here show that duocarmycin analogues **3** and **4** do not exert their cytotoxicity through the alkylation of ALDH1A1, since there is no correlation between the abundance or alkylation of this protein and the observed cytotoxic effects, and since the compounds lack the required potency and binding selectivity for one enantiomer in this interaction. Although ABPP with **3** labeled several other unidentified cytosolic proteins, these were only detected at concentrations much higher than those causing cytotoxicity, and none were alkylated with marked selectivity for the *S* enantiomer. Instead, the cytotoxicity of **3** and **4** can reasonably be explained through alkylation of DNA, given the demonstration that **3** can both alkylate and crosslink this

target. This explanation is consistent with the greatly superior potency of (*S*,*S*)-**3** compared to (*R*,*R*)-**3**, the sensitivity of a DNA-repair-deficient cell line to all four compounds, and the nuclear localization of the signal derived from a click reaction of (*S*)-**4** with a fluorescent dye. It also offers an explanation for the dependency of dimer cytotoxicity on the chain length separating the alkylating subunits [for (*S*,*S*)-**3**, $n = 3$ methylenes in the linking chain, $IC_{50} = 0.11$ pM; for $n = 4$ and 5, $IC_{50} = 9.0$ and 1.0 pM respectively].[4] As reported for other crosslinking agents incorporating duocarmycin analogues,[5,15] oscillating potency with linker chain length can be ascribed to matching the DNA base pair register—no obvious parallels for protein alkylation are apparent. Understanding the mechanism of action of duocarmycin analogues is important given the recent interest in their potential as anticancer agents,[4,16] but if ABPP is to be used in this role, then great care must be taken before attributing a biological function to any particular alkylated protein.

Received: October 18, 2012
Published online: April 24, 2013

[1] a) D. L. Boger, D. S. Johnson, *Angew. Chem.* **1996**, *108*, 1542 – 1580; *Angew. Chem. Int. Ed. Engl.* **1996**, *35*, 1438 – 1474; b) K. S. MacMillan, D. L. Boger, *J. Med. Chem.* **2009**, *52*, 5771 – 5780; c) N. Ghosh, H. M. Sheldrake, M. Searcey, K. Pors, *Curr. Top. Med. Chem.* **2009**, *9*, 1494 – 1524.
[2] a) D. L. Boger, D. S. Johnson, W. Yun, *J. Am. Chem. Soc.* **1994**, *116*, 1635 – 1656; b) A. Asai, S. Nagamura, H. Saito, *J. Am. Chem. Soc.* **1994**, *116*, 4171 – 4177.
[3] T. Wirth, K. Schmuck, L. F. Tietze, S. A. Sieber, *Angew. Chem.* **2012**, *124*, 2928 – 2931; *Angew. Chem. Int. Ed.* **2012**, *51*, 2874 – 2877.
[4] L. F. Tietze, J. M. von Hof, M. Müller, B. Krewer, I. Schuberth, *Angew. Chem.* **2010**, *122*, 7494 – 7497; *Angew. Chem. Int. Ed.* **2010**, *49*, 7336 – 7339.
[5] a) M. A. Mitchell, P. D. Johnson, M. G. Williams, P. A. Aristoff, *J. Am. Chem. Soc.* **1989**, *111*, 6428 – 6429; b) M. A. Mitchell, R. C. Kelly, N. A. Wicnienski, N. T. Hatzenbuhler, M. G. Williams, G. L. Petzold, J. L. Slightom, D. R. Siemieniak, *J. Am. Chem. Soc.* **1991**, *113*, 8994 – 8995.
[6] See the Supporting Information.
[7] A. Asai, S. Nagamura, H. Saito, I. Takahashi, H. Nakano, *Nucleic Acids Res.* **1994**, *22*, 88 – 93.
[8] T. R. Cech, *Biochemistry* **1981**, *20*, 1431 – 1437.
[9] J. M. Hinz, R. S. Tebbs, P. F. Wilson, P. B. Nham, E. P. Salazar, H. Nagasawa, S. S. Urbin, J. S. Bedford, L. H. Thompson, *Nucleic Acids Res.* **2006**, *34*, 1358 – 1383.
[10] a) W. R. Wilson, S. M. Stribbling, F. B. Pruijn, S. P. Syddall, A. V. Patterson, H. D. S. Liyanage, E. Smith, K. J. Botting, M. Tercel, *Mol. Cancer Ther.* **2009**, *8*, 2903 – 2913; b) F. W. Hunter, J. Wang, R. Patel, H.-L. Hsu, A. J. R. Hickey, M. P. Hay, W. R. Wilson, *Biochemical Pharmacol.* **2012**, *83*, 574 – 585.
[11] C. P. Guise, M. R. Abbattista, R. S. Singleton, S. D. Holford, J. Connolly, G. U. Dachs, S. B. Fox, R. Pollock, J. Harvey, P. Guilford, F. Doñate, W. R. Wilson, A. V. Patterson, *Cancer Res.* **2010**, *70*, 1573 – 1584.
[12] V. Neumeister, S. Agarwal, J. Bordeaux, R. L. Camp, D. L. Rimm, *Am. J. Pathol.* **2010**, *176*, 2131 – 2138.
[13] R. W. Storms, A. P. Trujillo, J. B. Springer, L. Shah, O. M. Colvin, S. M. Ludeman, C. Smith, *Proc. Natl. Acad. Sci. USA* **1999**, *96*, 9118 – 9123.
[14] J. S. Moreb, J. R. Zucali, B. Ostmark, N. A. Benson, *Cytometry Part B* **2007**, *72*, 281 – 289.
[15] M. Tercel, S. M. Stribbling, H. Sheppard, B. G. Siim, K. Wu, S. M. Pullen, K. J. Botting, W. R. Wilson, W. A. Denny, *J. Med. Chem.* **2003**, *46*, 2132 – 2151.
[16] M. Tercel, G. J. Atwell, S. Yang, A. Ashoorzadeh, R. J. Stevenson, K. J. Botting, Y. Gu, S. Y. Mehta, W. A. Denny, W. R. Wilson, F. B. Pruijn, *Angew. Chem.* **2011**, *123*, 2654 – 2657; *Angew. Chem. Int. Ed.* **2011**, *50*, 2606 – 2609.

